Versatile and Portable Cas12a-mediated Detection of Antibiotic Resistance Markers

Maryhory Vargas-Reyes[1,2], Roberto Alcántara[1,3,*], Soraya Alfonsi[3], Katherin Peñaranda[1,3], Dezemona Petrelli[3], Roberto Spurio[3], Monica J. Pajuelo[2], Pohl Milon[1,*]

[1]Biomolecules Laboratory, School of Biology, Faculty of Health Sciences, Universidad Peruana de Ciencias Aplicadas, Lima, Peru

[2]Laboratorio de Microbiología Molecular, Laboratorios de Investigación y Desarrollo, Facultad de Ciencias e Ingeniería, Universidad Peruana Cayetano Heredia, Lima, Peru

[3]School of Biosciences and Veterinary Medicine, University of Camerino, Camerino, Italy

[*]Correspondence: Pohl Milon: pmilon@upc.pe; Roberto Alcántara: roberto.alcantara@upc.pe

Keywords: Antibiotic Resistance Gene, Antimicrobial Resistance, Cas12a, *blaCTX*, *floR*, Integrase.

Abstract (217/250)

Antimicrobial resistance (AMR) is a global public health problem particularly accentuated in low- and middle-income countries, largely due to a lack of access to sanitation and hygiene, lack of awareness and knowledge, and the inadequacy of molecular laboratories for timely and accurate surveillance programs. This study introduces a versatile molecular detection toolbox (C12a) for antibiotic resistance gene markers using CRISPR/Cas12a coupled to PCR. Our toolbox can detect less than $3x10^{-7}$ ng of DNA (100 attoMolar) or 10^2

CFU/mL. High concordance was observed when comparing the C12a toolbox with sequenced genomes and antibiotic susceptibility tests for the *blaCTX-M-15* and *floR* antibiotic resistance genes (ARGs), which confer resistance to cefotaxime and other β-lactams, and amphenicols, respectively. C12a^{INT}, designed to detect the Integrase 1 gene, confirmed a high prevalence of the integrase/integron system in *E. coli* containing multiple ARGs. The C12a toolbox was tested across a wide range of laboratory infrastructure including a portable setup. When combined with lateral flow assays (LFA), C12a exhibited competitive performance, making it a promising solution for on-site ARG detection. Altogether, this work presents a collection of molecular tools (primers, crRNAs, probes) and validated assays for rapid, versatile, and portable detection of antibiotic resistance markers, highlighting the C12a toolbox potential for applications in surveillance and ARG identification in clinical and environmental settings.

Introduction

The discovery of antibiotics allowed control of pathogenic bacterial proliferation, enabling surgeries, treating infections, and boosting farm productivity, ultimately benefiting humans. Their use in clinical treatments has significantly increased life expectancy (1). However, the combination of excessive and inappropriate antibiotic use, complex ecological factors (2, 3), and horizontal gene transfer have favored the spread and selection of resistant strains (4, 5). Extended Spectrum Beta Lactamases (ESBLs) and amphenicol resistance are of particular concern for human and animal health. In Gram-negative bacteria, the *blaCTX-M-15* and *floR* antibiotic resistance genes (ARGs) confer resistance to β-lactam and

amphenicol antibiotics, used to treat infections in clinical and veterinary settings, respectively (6, 7). Both ARGs have been monitored in various environments such as hospitals, air, water, farms, soil, and wastewater (8)(Figure 1A). Monitoring *blaCTX-M-15* and *floR*, the most frequently detected variants within their respective classes, is essential for assessing the scale of their spread across populations and ecological systems (9–12).

At the molecular level, mobile genetic elements (MGEs) play a crucial role in the spread of antimicrobial resistance genes (ARG), due to their ability to physically move within different hosts, intra- or interspecies (13). In *Enterobacteriaceae*, like *E.coli*, Class 1 integrons are important contributors to ARG dissemination (14), and the most prevalent in clinical isolates (15–17) (Figure 1 B). Class 1 Integron consists of three coding modules: i) the *intI1* gene located at the 5' end, which codes for an integrase; ii) a recombinase site (*attI*) followed by an array of various gene cassettes; and; iii) a genome-integrated region at the 3' end, which varies between environmental and clinical Class 1 Integrons (18). The structure of the cassette array can be shaped by the selective pressure imposed by anthropogenic activities and could be used as an indicator of the presence of antibiotic-resistance genes. In addition to antibiotics, they are associated with resistance to disinfectants, heavy metals, and other pollutants (18). The detection of anthropogenic Class 1 Integron in environmental samples through the application of precise and affordable methods, is a necessary step to assess the impact of human activities and ecological genetic pollution (17).

Different methods for detecting antimicrobial resistance (AMR) are currently in use, with the most common being antimicrobial susceptibility testing (AST) and molecular

techniques such as qPCR and DNA sequencing (19, 20). However, there is a need for a tool that combines the speed of ARG detection provided by molecular methods with AST costs. Target pre-amplification followed by nucleic acid detection using CRISPR technology has shown promising results due to the high specificity, sensitivity, low costs, and speed of the assay (21). The molecular detection mechanism involves crRNA, a targeting sequence homologous to the gene of interest. Hybridization with the complementary target region activates Cas12a, which then engages in trans-cleaving activity, non-specifically cutting ssDNA (22). When using a fluorescence donor/quencher FRET pair placed into a ssDNA, this trans-cleaving activity leads to an increase in fluorescence (23) (Figure 1C).

Here, we use CRISPR technology to develop the C12a toolbox, a set of molecular tools and assays to detect genetic elements conferring antibiotic resistance or involved in ARG propagation. C12a^{bCTX} and C12a^{FLO} detect *blaCTX-M-15* and *floR* genes, respectively, while C12a^{INT} detects the Class 1 integrase gene as a rapid indicator of the potential presence of other ARGs. We also provide crRNAs designed for detecting ARGs commonly associated with MGEs. The C12a toolbox was optimized for three different laboratory setups (Figure 1C) including high-, and low-equipped in addition to a portable setting. Altogether, the C12a toolbox developed here entails a set of novel molecular assays to achieve rapid and efficient ARG detection.

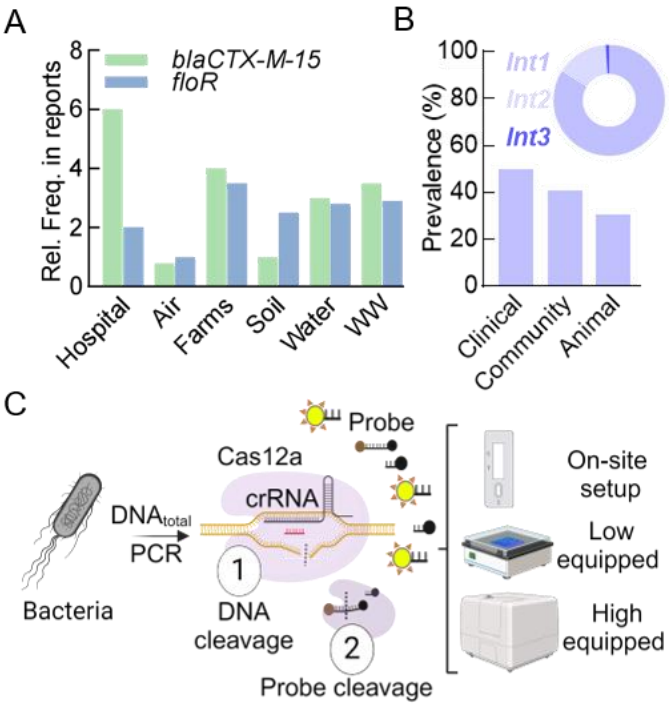

Figure 1. *blaCTX* and *floR* epidemiological context and the C12a rationale. (A) Frequency distribution of *blaCTX-M-15* and *floR* across various environments, based on publication frequency from 1990 to 2020 (8). WW: wastewater. **(B)** Prevalence of the Class 1 Integron across clinical, community, and animal settings (15, 24). The pie chart shows integron prevalence in clinical isolates (25). **(C)** Scheme showing the C12a toolbox and the molecular mechanism of Cas12a-mediated detection, highlighting signal development, versatility, and portability.

Materials and Methods

The **Extended Methods in the Supplemental Material file** provides details on biological components, microbiology assays, and bioinformatic analysis.

Assay Optimization

DNA amplification and analysis: PCR conditions for amplifying the *blaCTX-M-15* and *floR* targets included an initial denaturation at 95°C for 3 minutes, followed by 30 cycles of denaturation at 95° for 30 sec, annealing at 59°C for 30 sec, extension at 72°C for 30 sec,

and a final extension at 72°C for 5 minutes. For the *intI1* gene target, an annealing temperature of 56°C was used. The master mix included 2 ng/µl Taq DNA polymerase, 0.2 µM primers in the RPB1X buffer (Table S1), and DNA concentrations ranging from 1 to 10 ng/µl, in a final volume of 20 µl. PCR products were visualized using agarose gel electrophoresis (Cat # CSL-AG500, Cleaver Scientific). Gel concentrations were optimized at 1.7% for all genes. Electrophoresis was performed in 1X TBE buffer (Table S1) at 80 V for 1 hour. A 5 µl aliquot of PCR product was mixed with 1 µl of 6X Trick-Track – SYBR Gold (Cat # R1161, ThermoFisher), and loaded onto the agarose gel. A 100 bp molecular weight marker (Cat # SM0242, Thermo Scientific) was included. Agarose gels were imaged with a gel documentation system using the Sybergold option (Gel Doc-BioRad). Band intensity was quantified by calculating the area under the curve (AUC) with Gel Analyzer v23 (www.gelanalyzer.com).

crRNA/Cas12a-mediated detection: the crRNA was refolded through a sequential incubation, first at 65°C for 10 minutes, followed by 10 minutes at 25°C. The crRNA/Cas12a complex (0.1 µM Cas12a, 0.15 µM crRNA, and 2 µM FAM probe [6-FAM/TTATT/3IABkFQ]) was incubated in CRB1 buffer (Table S1) in the dark for 10 minutes. Afterward, 5 µl of amplification reaction was mixed with 10 µl of the crRNA/Cas12a complex in CRB2 buffer (Table S1) in a black 96-well plate (Cat #23710, ThermoFisher), in a volume of 100 µl. Fluorescence was measured using a plate reader (Synergy H1, BioTek Instruments) with excitation at 491 nm and emission at 525 nm.

Template and Mg2+ optimization: A six-point curve of total DNA was established using a serial dilution ranging from 1 ng/µl to 10-5 ng/µl to optimize the template concentration. A

magnesium concentration curve was performed, ranging from 7.5 mM to 25 mM in CRB1 buffer (Table S1), using 2 ng/µl of genomic DNA and 30 amplification cycles.

LoB and LoD determination: Ten susceptible *E.coli* isolates (negative controls) were evaluated to determine the LoB (Limit of Blank) as the cut-off ratio, using the formula LoB = Avg_NF_{NTC} + 2 SD (where "Avg" is average NF_{ntc} values, and "SD" is standard deviation)(26). The LoD (Limit of Detection) was determined for both amplification products and bacterial cell counts for the *blaCTX-M-15* and *floR* targets. Amplicons were purified using the Oligo Clean Kit (Cat # D4060, Zymo Research). Serial ten-fold dilutions of the purified product, from 1 aM to 10 nM, were prepared, resulting in 10 dilution points. The LoD was then calculated using the formula LoD = LoB + 2 (SD_low concentration sample) (26). For the bacterial cell LoD determination, a curve was generated using an *E. coli* isolate positive for the antimicrobial resistance gene. Starting from a cell density of 0.5 McFarland, 7 ten-fold dilutions were prepared in duplicate. One set of dilutions was plated on LB agar plates, while the other set was analyzed using the CRISPR/Cas12a method.

Lateral Flow Assay (LFA): Target genes were amplified by PCR from a small set (N = 14) of stored purified DNA from stool samples and detected using the described Cas12a assays. After denaturation and refolding of 0.15 µM crRNA, the crRNA/Cas12a complex (0.2 µM Cas12 and 5 µM of probe [6-FAM/TTATTATT/BIOTIN]) was mixed in CRB1 buffer and incubated in the dark for 10 minutes. Then, 10 µl of the crRNA/Cas12a complex was mixed with 6 µl of PCR products and CRB2 buffer, in a volume of 95 µl. This mixture was incubated for 30 minutes in the dark. Next, polyethylene glycol was added to a final concentration of 5% (Cat # 25322-68-3, Merck), and a LFA strip (Cat # 3822-9000,

Milenia Biotec GmbH) was submerged in each mixture. The signal on the strips was detected after 5-10 minutes.

Results

C12a Development

To define the optimal sets of primers, we first compared 61 *blaCTX-M-15* sequences and 46 *floR* sequences from *E. coli* isolates available in GenBank (27) (Supplementary Dataset 1 and Dataset 2, respectively). Based on the consensus sequences for each gene, we selected two primer sets for *blaCTX-M-15* and one for *floR* (Table S2) (Figure 2A), which amplify efficiently a DNA region containing both the crRNA complementary sequence and a PAM region (TTTN) (28) (Figure S1). Agarose gel electrophoresis revealed defined bands at 216 bp and 270 bp for *blaCTX-M-15,* and *floR* amplicons, respectively. Negative controls showed no DNA amplification, as determined by gel electrophoresis (Figure S2). Amplicons were sequenced to confirm the presence of the expected target DNA for each gene (Table S3). To optimize the crRNA/Cas12a reaction, two candidate crRNAs for each target gene were designed (Table S2). To determine sensitivity parameters, a test carried out using increasing Mg^{2+} concentrations revealed an optimal value of 20 mM (Figure S3), which was used in all assays. Both *blaCTX-M-15* and *floR* amplicons were recognized by the crRNA/Cas12a complex, resulting in an increase in fluorescence over time. However, primer set 2, combined with $crRNA^{CTX-2}$, showed greater fluorescence intensity compared to $crRNA^{CTX-1}$. For *floR*, $crRNA^{FLO-1}$ exhibited a higher fluorescence change than $crRNA^{FLO-2}$ (Figure S1). Notably, regardless of template concentration, $crRNA^{CTX}$

consistently generated a fluorescence signal faster than the *floR* crRNAs (Figure 2B and Figure S1). Thus, the selected crRNAs for *blaCTX-M-15* and *floR* were $crRNA^{CTX-2}$ and $crRNA^{FLO-1}$, respectively.

For better comparison with previous reports, this study used a fluorescence signal normalized to the no-template control (NTC), indicated as NF_{NTC} (a.u.). To calculate NF_{NTC}, each raw fluorescence data point was divided by its corresponding data point from the NTC (Figure 2C). For both target genes, the measured NF_{NTC} for positive controls was 4- to 14-fold higher than for negative controls. Specifically, for the *blaCTX-M-15* gene, positive samples exhibited an NF_{NTC} of at least 14-fold, while negative samples showed values similar to the NTC, with NF_{NTC} values near 1. Similarly, for the *floR* gene, positive samples showed a 4-fold increase in NF_{NTC} compared to negative controls (Figure 2C and Figure S1).

For *blaCTX-M-15* evaluation, the $C12a^{bCTX}$ detection system was used, which incorporates the primer set 2 and $crRNA^{CTX-2}$ (Table S2). On the other hand, the presence of *floR* was evaluated using the $C12a^{FLO}$ detection system using the primer set 1 in combination with $crRNA^{FLO-1}$ (Table S2).

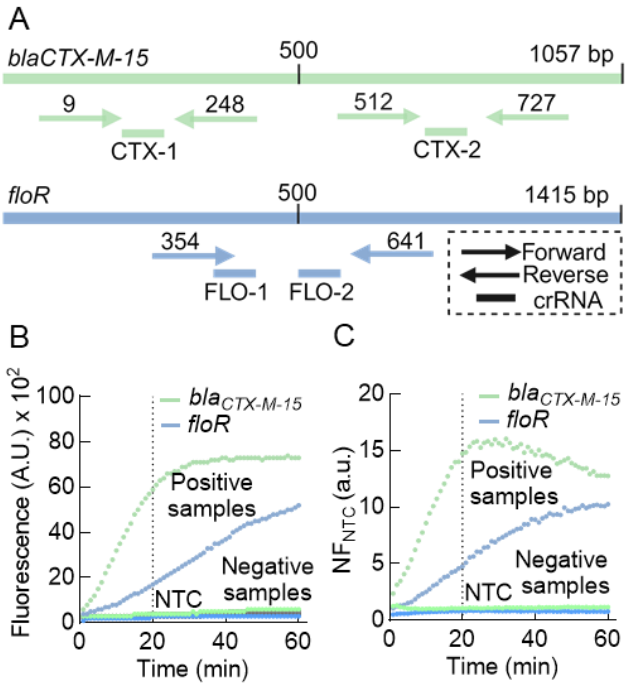

Figure 2. Experimental setup for CRISPR/Cas12a-based assay development. **(A)** Primers and crRNA location on *blaCTX-M-15* and *floR* gene targets, ensuring coverage of PAM regions and complementary crRNA areas. **(B)** Example of raw fluorescence readouts from CRISPR/Cas12a assays, showing a time-dependent increase of the signal. Positive and negative controls, alongside the Non-Template Control (NTC), are represented to illustrate the assay's ability to differentiate samples with or without ARGs. **(C)** Example of normalized fluorescence ratio NF_{NTC} (a.u.) over time. In **(B)** and **(C),** the dotted line indicates the 20-minute detection point, selected as the cut-off reading time for analysis.

C12a Analytical Sensitivity

Two key analytical parameters describe a laboratory assay for analyte detection: the limit of blank (LoB; also referred to as the cut-off) and the limit of detection (LoD). The LoB was determined using total DNA from ten susceptible *E. coli* isolates. The LoB was calculated as the average NF_{NTC} plus the standard deviation multiplied by a confidence factor (LoB=Avg + c x SD, where c=2) (26). The average NF_{NTC} values for negative samples

using C12a^{bCTX} or C12a^{FLO} were 1.04 ± 0.02 and 0.94 ± 0.02 after 20 minutes of incubation (Figure S4). Thus, the resulting LoB values were 1.07 NF_{NTC} (a.u.) for C12a^{bCTX} and 0.97 NF_{NTC} (a.u.) for C12a^{FLO}. Based on these values, we can state that 95.45% of the values below the determined LoB were likely to be classified as nonspecific background signals (i.e., signals in the absence of the analyte) (Figure S4).

To estimate the LoD for both detection systems, purified and quantified amplicons were tested at increasing concentrations (from 1 attoM to 10 nanoM). Averaged NF_{NTC} (a.u.) values, measured at 10-minute intervals were used to define the lowest detectable target concentration and the shortest reaction time. The LoD was calculated for each time interval, allowing the estimation of LoD as a function of incubation time (Figure 3A). The time dependence indicates that after 21 minutes for C12a^{bCTX} and 17 minutes for C12a^{FLO}, the LoD reached half of its maximum value, suggesting that a 20-minute reaction time is a good compromise between assay speed and analytical sensitivity. The calculated LoD for C12a^{bCTX} and C12a^{FLO} at 20 minutes was 70 aM and 50 aM, respectively (Figure 3B). Taking NF_{NTC} values at times shorter than 20 minutes would result in a tenfold loss in sensitivity (Figure 3A).

We then assessed the analytical sensitivity of the CRISPR/Cas12a system in terms of the number of cells carrying the resistance genes (Figure 3C). Fresh bacterial cultures of *E.coli* ATCC25922 ranging from 3 to $3x10^6$ CFU/mL were used (Figure S5). Non-linear fitting of the NF_{NTC} dependence on cell number (CFU) allowed the calculation of the LoD. C12a^{bCTX} reliably detected the *blaCTX-M-15* gene at 77 CFU/mL, while C12a^{FLO} required 173 CFU/mL to detect the *floR* gene (Figure 3C). Both ARG detection systems showed low LoB values and enabled the detection of extremely low concentrations of the target DNA

(LoDs) with a 20-minute incubation at room temperature. Additionally, the lowest target concentration that could be empirically detected for the two target genes, was 10 to 100 times lower compared to gel electrophoresis analysis of PCR amplification (Figure 3D,E, and Figure S6). Altogether, the detection and sensitivity performance of C12a^{bCTX} and C12a^{FLO} provide a solid foundation for testing the detection systems on a larger number of samples (see below).

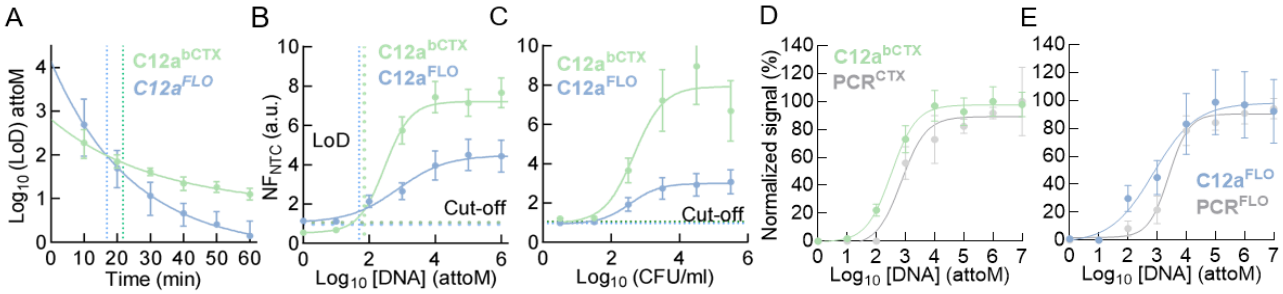

Figure 3. C12a^{bCTX} and C12a^{FLO} Limit of Detection (LoD). (A) Time-resolved determination of LoD values for both ARGs Cas12a reactions, plotted on a logarithmic scale. The graph illustrates the LoD decrease for C12a^{bCTX} and C12a^{FLO} over incubation time, with dotted lines marking the time-point when the LoD reaches half its maximum value. **(B)** Normalized fluorescence ratio as a function of target concentration for ARG detection assays. The X-axis dotted lines represent the LoD value calculated at 20 minutes, while the Y-axis dotted lines represent NF_{NTC} LoB (cutoff). **(C)** Normalized fluorescence ratio over bacterial cell concentration for both C12a assays. The dotted lines indicate average NF_{NTC} cut-off values of 1.04 and 0.94 for C12a^{bCTX} and C12a^{FLO}, respectively. **(D)** Normalized assay signals across target concentrations for C12a^{bCTX} detection compared to PCR-based detection evaluated by gel electrophoresis. The fluorescent ratio for the Cas12a reaction and electrophoresis gel band intensity, recorded as Area Under the Curve (AUC) values, are normalized as percentages to the highest value. **(E)** Same as (D), but for C12a^{FLO}. Error bars represent standard deviations from 3 replicates.

C12a^{bCTX} and C12a^{FLO} performance in E. coli isolates

To assess the presence of antibiotic resistance genes (ARGs) and the phenotypic resistance in *E. coli* isolates, two distinct assays were conducted: (i) molecular detection using the C12a toolbox and (ii) antimicrobial susceptibility testing (AST). A total of 32 *E. coli* isolates were selected, each containing either the *blaCTX-M-15* gene, the *floR* gene, or neither, from a previously published sample repository (NIH R01AI108695-01A1) (29). Of these, 15 samples were tested for beta-lactam resistance and 17 for amphenicol resistance (Table S4), using the combined disk (CD) test and broth microdilution for minimum inhibitory concentration (MIC) determination, respectively. Finally, the C12a assay was applied to all samples of the collection.

All isolates positive to the *blaCTX-M-15* gene (7 samples) were ESBL producers, confirming the resistance to beta-lactam antibiotics. Similarly, resistant isolates harboring the *floR* gene (11 samples) exhibited MIC values ranging from 256 to 128 µg/mL, while susceptible isolates (6 samples) had MIC values below 32 µg/mL (30) (Table S4). When assessing the performance of C12a^{bCTX} and C12a^{FLO} systems, NF_{NTC} values for ARG-positive samples ranged from 11 to 16 for C12a^{bCTX} and 3 to 4.5 for C12a^{FLO} after 20 minutes of incubation, indicating the detection of the target genes. In contrast, ARG-negative samples showed no NF_{NTC} values higher than 1.0 with either C12a assay, indicating the absence of the target genes (Figure 4A-B). A strong concordance was observed between the presence of resistance genes using the C12a toolbox, genetic data, and the phenotypic resistance determined by AST assays (Figure 4C-D).

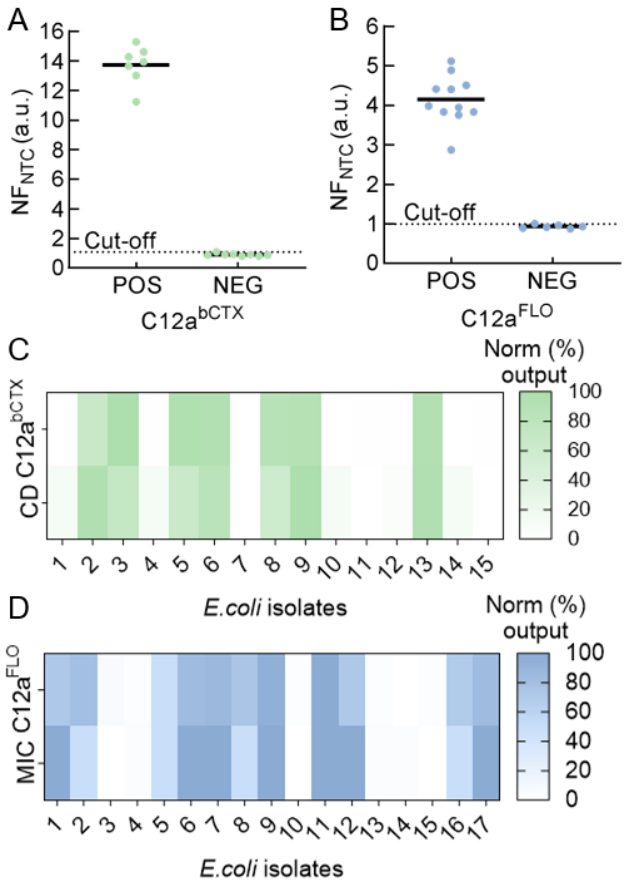

Figure 4. C12a^{bCTX} and C12a^{FLO} comparison with AST methods. (A) Distribution of *blaCTX-M*-15 in 17 isolates tested using the C12a^{bCTX} assay. The dotted line represents the LoB at 1.1. **(B)** Similar to (A), but for the C12a^{FLO} assay. The dotted line indicates the LoB at 1.0. **(C)** Heat map comparison of the C12a^{bCTX} assay with the disk diffusion test for AMR (CD). Results were normalized to percentages, using the maximum value obtained for each dataset as 100%. **(D)** Similar to (C) but for the C12a^{FLO} assay with microdilution test (MIC), showing that *floR* positive samples were phenotypically resistant to florfenicol.

C12a^{INT} detects the intI1 gene

The spread of ARGs can be mediated by Class 1 Integron, which is known to host genes conferring resistance to aminoglycosides, sulfonamides, beta-lactams, and trimethoprim. The modularity and versatility of the Ca12a toolbox could allow a rapid adaptation to detect

other genetic elements relevant to the AMR problem. Bioinformatic analysis of ARG-positive *E. coli* isolates (Fig. 4 A) revealed that 77.77% (14/18) contained the *intI1* gene, encoding Integrase I. Nearly all integrase-positive isolates also carried a cassette array (78.57%), indicated by the presence of the attC recombination sites. Three isolates had *intI1* integrase but lacked a cassette array, while one lacked the integrase but carried a cassette array. For samples carrying the Class 1 integron, deeper bioinformatic analysis was performed on 18 genomes, to identify the ARG genes present in the cassette array. Genes conferring resistance to aminoglycosides, trimethoprim, phenicols, lincosamide and sulfonamides were the most prevalent, with frequencies of 91.67%, 75%, 33%, 25%, and 16.67%, respectively. Additionally, genes conferring tolerance to disinfectants such as *qacE* were observed in 5 isolates (41.67%) (Figure 5A). The *in silico* analysis revealed that transposons localized near Class 1 Integron, were probably involved in the mechanism of acquisition and transfer of the observed cassette array. Neither *blaCTX-M-15* nor *floR* genes were detected as part of the cassette array in any of the analyzed isolates (Table S5). Thus, we designed a collection of primers and crRNAs for detecting the representative ARGs for each antibiotic family (Table S6) and for the *intI1* gene. From this collection, we further tested the C12a using the $C12a^{INT}$ assay and the *E. coli* isolates library. Agarose gel electrophoresis revealed defined bands at 146 bp only for *intI-1* positive samples using a reported set of primers (31) (Figure S7). Among the three candidate crRNAs, $crRNA^{int3}$ showed better NF_{NTC} values at 20 minutes reaction time under standardized C12a reaction conditions (Figure 5B). Using the $C12a^{INT}$, we detected the presence of the *intI1* gene in 16 out of 18 ARG-positive samples (Figure 5C). Detection of *intI1* could indicate the presence of other resistances frequently associated with Class 1 Integron (17, 32, 33). Furthermore, although *intI1* could be a good predictor of resistance to some antibiotic classes, direct

detection of the ARG may be preferable for certain setups Here we provide a set of primers and crRNAs designed by bioinformatic analysis with the aim to detect the most prevalent ARGs found in the Class 1 integron cassette array (Table S6), a target region suitable for CRISPR/Cas technology. Therefore, this could be a solid starting point for studies aiming to direct detection of relevant ARGs.

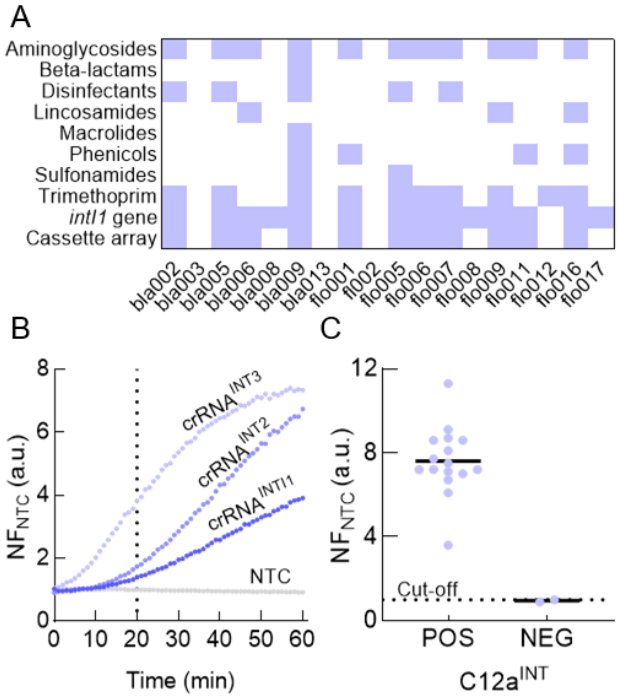

Figure 5. C12a^{INT} detects the *intI1* gene, a potential marker of multidrug-resistant *E.coli*. (A) Heat map summarizing the antibiotic resistance genes related to different antibiotic families identified within the Class 1 integron cassette array of the ARG-positive *E. coli* isolates used in this study. ARGs were identified by bioinformatic analysis of sequencing data (BioProject number PRJNA821865) using CARD. **(B)** Time-course of normalized fluorescence development for the C12a^{INT} assay with three crRNA designed to detect the *intI1* gene. The X-axis dotted line represents the incubation time used for further analysis. **(C)** CRISPR-Cas detection of *intI1* gene in 18 ARG-positive isolates tested using the C12a^{INT} assay. The dotted line represents the LoB at 1.0.

Efficient C12a-mediated ARGs detection in different Lab setups

Differences in equipment availability and portability may impact the analytical performance of the C12a detection toolkit. To address this, we adapted our detection assays to three laboratory setups: i) Low-C12a–for low-equipped labs with minimal tools, such as a thermocycler and transilluminator, for qualitative readouts; ii) OnSite-C12a–for portable setups with equipment-free readouts using the Lateral Flow Assay (LFA) platform and transportable workstation like BentoLab®, and iii) High-C12a– for a high-equipped setup with a multimode microplate reader for precise quantitative analysis, as used here for the C12a validation (Figure 6).

Fourteen purified total DNA available from the stool sample repository (BioProject number PRJNA821865) were assessed with the C12a^{bCTX} (7 samples) and C12a^{FLO} (7 samples) using all three laboratory set-ups. Using Low-C12a^{bCTX}, direct visualization of fluorescence allowed detection for the five positive samples. Negative samples did not show any fluorescence signal. When using Low-C12a^{FLO}, six samples tested positive by direct observation (Figure 6A). The high-equipped setup showed that C12a^{bCTX} detected *blaCTX-M-15* in five samples, and two samples tested negative, respectively. All positive samples showed NF_{NTC} (a.u.) values exceeding 6 within 20 minutes. Similarly, for the C12a^{FLO}, NF_{NTC} (a.u.) values surpassing 3 were recorded at 20 minutes (Figure 6B). When using a portable setup with OnSite-C12a^{bCTX} and OnSite-C12a^{FLO}, the presence of the ARG is indicated by the appearance of two bands: the first is the C line (control) and an additional band that is the T line (test), which can display an intensity equal to or greater than that of the C line. Both bands were observed exclusively in the positive samples for both ARG evaluated (Figure 6C). Under our experimental conditions, no difference in detection

performance was observed in all three setups evaluated. Although the sample size was limited, these results provide an initial indication that our toolbox demonstrates sufficient analytical sensitivity for direct ARG detection in total DNA samples across different laboratory setups.

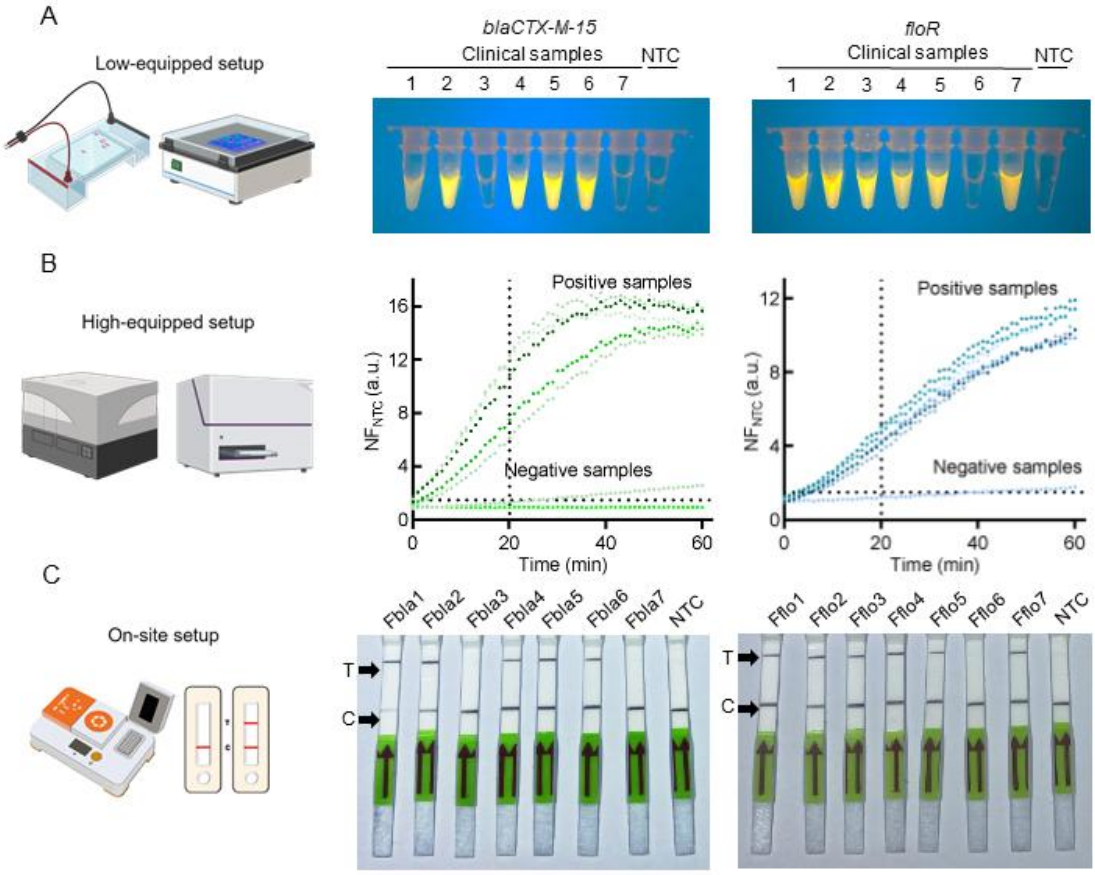

Figure 6. C12a application across different laboratory setups. (A) *blaCTX-M-15* and *floR* detection in a low-equipped laboratory setup. Fluorescence was observed by direct visualization only for ARG-positive samples, photographed using a smartphone camera with default settings using a blue light transilluminator. **(B)** Similar to (A), but for a high-equipped laboratory. NF_{NFC} (a.u.) values were measured over 60 minutes with a 20-minute detection cutoff. The Y-axis dotted line represents an average NF_{NTC} cut-off value of 1.0. **(C)** Similar to (A), but for an On-site setup. Detection by LFA strips at 15 minutes

incubation, where the T band is positive and C the quality control. NTC refers to non-template control.

Discussion

Antimicrobial resistance is a growing threat beyond clinical settings, confirmed by the detection of AMR pathogenic bacteria and mobile genetic elements in the environment, including anthropogenic integrons in *Enterobacteriaceae* (33). The detection of *blaCTX-M-15* and *floR* gene is of increasing importance due to their widespread distribution in antimicrobial resistance (Figure 1A). *blaCTX-M-15* is one of the most prevalent extended-spectrum β-lactamase (ESBL) genes globally, conferring resistance to a wide range of β-lactam antibiotics, including third-generation cephalosporins (34). Its widespread dissemination among Enterobacteriaceae, particularly *Escherichia coli*, poses a serious threat to public health by limiting treatment options for bacterial infections. Similarly, the *floR* gene confers resistance to amphenicols like florfenicol, an antibiotic used in veterinary medicine (35). The presence of these genes facilitates the survival and spread of multidrug-resistant bacteria in various environments, making their detection crucial for effective surveillance and control measures.

Therefore, our research presents an optimized molecular detection toolbox for two of the most widespread genes conferring resistance to beta-lactams (*blaCTX-M-15)* and amphenicols (*floR*) and *Int1* integrase, using the CRISPR-Cas technology. This toolbox is composed of a collection of primers, crRNAs, and well-defined protocols to be applied in laboratories with different equipment availability. Detection of *blaCTX-M-15* and *floR* with C12a^{bCTX} and C12a^{FLO}, display distinctive features, such as incubation times as short as 20

minutes and competitive low limits of detection, that make them suitable for various applications. The analytical performance of Cas-based assays competes well with established molecular techniques; yet, they are simpler, faster, and more versatile. Our C12a detection systems can recognize the target genes with similar analytical sensitivity as commercial qPCR kits for ARGs detection (36). Furthermore, they have proven to be robust and effective with a limit of detection in the range of 75 to 180 bacterial cells per reaction, as the limit of detection, indicating high sensitivity.

Anthropogenic integrons in *Enterobacteriaceae* are frequently associated with multidrug resistance and are influenced by human activities (17, 37). Global studies have frequently reported the widespread Class 1 integron/integrase systems carrying resistances to aminoglycosides, sulfonamides, beta-lactams, and trimethoprim. Research conducted in wastewater treatment plants (WWTPs) has also demonstrated that the Class 1 integron/integrase system can be a potential indicator of ARGs abundance, making it a promising indicator for environmental surveillance (38). Furthermore, various studies indicate that ARGs can be acquired from animal sources through horizontal gene transfer, illustrating complex AMR dissemination pathways (39). For instance, genetic analyses have shown similarities in plasmids carrying the *floR* gene in *E. coli* strains from both human and livestock samples, suggesting a possible zoonotic vector for ARG transmission (7, 40). This hypothesis is further supported by studies linking contaminated poultry meat consumption to potential horizontal gene transfer of *floR* to human commensals (41). In this scenario, our C12a toolbox has the potential to be adopted and used as a rapid surveillance system in the aforementioned situations. Our findings, in agreement with previous studies, show that C12a^{INT} finds that *E.coli* isolates carrying the *intI1* gene are also positive for *blaCTX-M-15*.

However, bioinformatic analysis shows that *blaCTX-M-15* is not located within the mobile cassette array. Similarly, although a high correspondence between the *floR* and *intI1* presence, *floR* was not found within the integron cassette array. A molecular rationale behind these observations remains to be discovered. Mechanisms of DNA shuffling involving mobile genetic elements, like transposons or insertion sequences may facilitate the acquisition, loss, and spread of ARGs within the integron cassette array.

Although our study involved a limited number of *E. coli* isolates, the results perfectly conform with those obtained from established molecular and microbiological tests, indicating a high degree of reliability. The high specificity of C12a systems aligns with other molecular detection methods, thanks to the dual recognition steps mechanism, which involves both primer selection and crRNA binding. Of special interest, is the implementation of Cas12a systems into a large range of laboratory equipment availability. The performance of our C12a detection systems was consistent across all setups (Figure 6), showing low sensitivity losses (<10-fold) in low-equipped or portable setups as compared to a high-end laboratory. Remarkably, the portable system, albeit using lateral flow assay (LFA), that represents a leap toward field-ready applications, allowing direct and on-site ARG detection. The development of a simplified detection system for ARGs is crucial for investigating AMR across a spectrum of contexts, from clinical settings to environmental and veterinary surveillance. The technical features of our toolbox are valuable because they enable accurate, consistent, and cost-effective monitoring/surveillance efforts. These aspects are particularly beneficial for resource-limited settings lacking an adequate, cutting-edge, laboratory infrastructure.

Ethics

The *E. coli* isolates used in this study were derived from a strain collection of a longitudinal study approved by the ethics committee of Universidad Peruana de Cayetano Heredia (UPCH, SIDISI: 65178).

Authors Contribution

M.V-R., R.A., M.P., and P.M. conceived the project. M.V-R., R.A., and P.M. designed experiments. M.V-R., and S.A. performed experiments. M.V-R., R.A., and P.M. analyzed the data. M.V-R, R.A., K.P., and P.M. elaborated figures, and tables. R.S. and D.P. helped with data interpretation. M.V-R., R.A., S.A., K.P., and P.M. wrote the manuscript with the input of D.P., R.S., and M.P.

Disclosure of interest

The authors report there are no competing interests to declare.

Funding and acknowledgments

This work was supported by the PROCIENCIA program of CONCYTEC (Consejo Nacional de Ciencia, Tecnología e Innovación Tecnológica) with grant agreement

PE501079419-2022 to PM. Proof-of-concept was achieved with funding provided by the Universidad Peruana de Ciencias Aplicadas (C-004-2021-2) granted to RA.

This work has received funding from the European Union's Horizon 2020 research and innovation program under the Marie Sklodowska-Curie grant agreement No 872869, supporting the international mobility of RA, SA, KP, PM, and RS. Additionally, this work received funding from the Fogarty International Center, National Institutes of Health (D43TW001140), supported MP.

We are very thankful to Dr. Maya Nadimpalli for promptly providing sequencing data of the *E. coli* isolate collection used in this study.

References

1. Hutchings M, Truman A, Wilkinson B. 2019. Antibiotics: past, present and future. Curr Opin Microbiol 51:72–80.

2. Lipsitch M, Samore MH. 2002. Antimicrobial Use and Antimicrobial Resistance: A Population Perspective - Volume 8, Number 4—April 2002 - Emerging Infectious Diseases journal - CDC. Emerg Infect Dis 8:347–354.

3. Huijbers PMC, Blaak H, Jong MCM de, Graat EAM, Vandenbroucke-Grauls CMJE, Husman AM de R. 2015. Role of the Environment in the Transmission of Antimicrobial Resistance to Humans: A Review. Environ Sci Technol 49:11993–12004.

4. Wintersdorff CJH von, Penders J, Niekerk JM van, Mills ND, Majumder S, Alphen LB van, Savelkoul PHM, Wolffs PFG. 2016. Dissemination of Antimicrobial Resistance in Microbial Ecosystems through Horizontal Gene Transfer. Front Microbiol 7:173.

5. Samreen, Ahmad I, Malak HA, Abulreesh HH. 2021. Environmental antimicrobial resistance and its drivers: a potential threat to public health. J Glob Antimicrob Resist 27:101–111.

6. Ramadan AA, Abdelaziz NA, Amin MA, Aziz RK. 2019. Novel blaCTX-M variants and genotype-phenotype correlations among clinical isolates of extended spectrum beta lactamase-producing Escherichia coli. Sci Rep 9:4224.

7. Li P, Zhu T, Zhou D, Lu W, Liu H, Sun Z, Ying J, Lu J, Lin X, Li K, Ying J, Bao Q, Xu T. 2020. Analysis of Resistance to Florfenicol and the Related Mechanism of Dissemination in Different Animal-Derived Bacteria. Front Cell Infect Microbiol 10:369.

8. Zhuang M, Achmon Y, Cao Y, Liang X, Chen L, Wang H, Siame BA, Leung KY. 2021. Distribution of antibiotic resistance genes in the environment. Environ Pollut 285:117402.

9. Rangama S, Lidbury IDEA, Holden JM, Borsetto C, Murphy ARJ, Hawkey PM, Wellington EMH. 2021. Mechanisms Involved in the Active Secretion of CTX-M-15 β-Lactamase by Pathogenic Escherichia coli ST131. Antimicrob Agents Chemother 65:10.1128.

10. Negeri AA, Mamo H, Gahlot DK, Gurung JM, Seyoum ET, Francis MS. 2023. Characterization of plasmids carrying blaCTX-M genes among extra-intestinal Escherichia coli clinical isolates in Ethiopia. Sci Rep 13:8595.

11. Gundran RS, Cardenio PA, Villanueva MA, Sison FB, Benigno CC, Kreausukon K, Pichpol D, Punyapornwithaya V. 2019. Prevalence and distribution of blaCTX-M, blaSHV, blaTEM genes in extended- spectrum β- lactamase- producing E. coli isolates from broiler farms in the Philippines. BMC Vet Res 15:227.

12. Ying Y, Wu F, Wu C, Jiang Y, Yin M, Zhou W, Zhu X, Cheng C, Zhu L, Li K, Lu J, Xu T, Bao Q. 2019. Florfenicol Resistance in Enterobacteriaceae and Whole-Genome Sequence Analysis of Florfenicol-Resistant Leclercia adecarboxylata Strain R25. Int J Genom 2019:9828504.

13. Tokuda M, Shintani M. 2024. Microbial evolution through horizontal gene transfer by mobile genetic elements. Microb Biotechnol 17:e14408.

14. Zhang S, Abbas M, Rehman MU, Huang Y, Zhou R, Gong S, Yang H, Chen S, Wang M, Cheng A. 2020. Dissemination of antibiotic resistance genes (ARGs) via integrons in Escherichia coli: A risk to human health. Environ Pollut 266:115260.

15. Halaji M, Feizi A, Mirzaei A, Ebrahim-Saraie HS, Fayyazi A, Ashraf A, Havaei SA. 2020. The Global Prevalence of Class 1 Integron and Associated Antibiotic Resistance in Escherichia coli from Patients with Urinary Tract Infections, a Systematic Review and Meta-Analysis. Microb Drug Resist 26:1208–1218.

16. Deng Y, Bao X, Ji L, Chen L, Liu J, Miao J, Chen D, Bian H, Li Y, Yu G. 2015. Resistance integrons: class 1, 2 and 3 integrons. Ann Clin Microbiol Antimicrob 14:45.

17. Corno G, Ghaly T, Sabatino R, Eckert EM, Galafassi S, Gillings MR, Cesare AD. 2023. Class 1 integron and related antimicrobial resistance gene dynamics along a complex

freshwater system affected by different anthropogenic pressures. Environ Pollut 316:120601.

18. Gillings MR, Gaze WH, Pruden A, Smalla K, Tiedje JM, Zhu Y-G. 2015. Using the class 1 integron-integrase gene as a proxy for anthropogenic pollution. ISME J 9:1269–1279.

19. Abramova A, Berendonk TU, Bengtsson-Palme J. 2023. A global baseline for qPCR-determined antimicrobial resistance gene prevalence across environments. Environ Int 178:108084.

20. Abramova A, Karkman A, Bengtsson-Palme J. 2024. Metagenomic assemblies tend to break around antibiotic resistance genes. BMC Genom 25:959.

21. Li S-Y, Cheng Q-X, Wang J-M, Li X-Y, Zhang Z-L, Gao S, Cao R-B, Zhao G-P, Wang J. 2018. CRISPR-Cas12a-assisted nucleic acid detection. Cell Discov 4:20.

22. Chen JS, Ma E, Harrington LB, Costa MD, Tian X, Palefsky JM, Doudna JA. 2018. CRISPR-Cas12a target binding unleashes indiscriminate single-stranded DNase activity. Science 360:eaar6245.

23. Broughton JP, Deng X, Yu G, Fasching CL, Servellita V, Singh J, Miao X, Streithorst JA, Granados A, Sotomayor-Gonzalez A, Zorn K, Gopez A, Hsu E, Gu W, Miller S, Pan C-Y, Guevara H, Wadford DA, Chen JS, Chiu CY. 2020. CRISPR–Cas12-based detection of SARS-CoV-2. Nat Biotechnol 38:870–874.

24. Dehkordi MK, Halaji M, Nouri S. 2020. Prevalence of class 1 integron in Escherichia coli isolated from animal sources in Iran: a systematic review and meta-analysis. Trop Med Heal 48:16.

25. Zarei-Yazdeli M, Eslami G, Zandi H, Kiani M, Barzegar K, Alipanah H, Mousavi SM, Shukohifar M. 2018. Prevalence of class 1, 2 and 3 integrons among multidrug-resistant Pseudomonas aeruginosa in Yazd, Iran. Iran J Microbiol 10:300–306.

26. Armbruster DA, Pry T. 2008. Limit of blank, limit of detection and limit of quantitation. Clin Biochem Rev 29 Suppl 1:S49-52.

27. Nadimpalli ML, Salvatierra LR, Chakraborty S, Swarthout JM, Cabrera LZ, Pickering AJ, Calderon M, Saito M, Gilman RH, Pajuelo MJ. 2024. Effects of breastfeeding on children's gut colonization with multidrug-resistant Enterobacterales in peri-urban Lima, Peru. Gut Microbes 16:2309681.

28. Stella S, Mesa P, Thomsen J, Paul B, Alcón P, Jensen SB, Saligram B, Moses ME, Hatzakis NS, Montoya G. 2018. Conformational Activation Promotes CRISPR-Cas12a Catalysis and Resetting of the Endonuclease Activity. Cell 175:1856-1871.

29. Pajuelo MJ, Noazin S, Cabrera L, Toledo A, Velagic M, Arias L, Ochoa M, Moulton LH, Saito M, Gilman RH, Chakraborty S. 2024. Epidemiology of enterotoxigenic

Escherichia coli and impact on the growth of children in the first two years of life in Lima, Peru. Front Public Heal 12:1332319.

30. Singer RS, Patterson SK, Meier AE, Gibson JK, Lee HL, Maddox CW. 2004. Relationship between Phenotypic and Genotypic Florfenicol Resistance in Escherichia coli. Antimicrob Agents Chemother 48:4047–4049.

31. Zhang Y, Lu J, Wu J, Wang J, Luo Y. 2020. Potential risks of microplastics combined with superbugs: Enrichment of antibiotic resistant bacteria on the surface of microplastics in mariculture system. Ecotoxicol Environ Saf 187:109852.

32. McGivern BB, McDonell RK, Morris SK, LaPara TM, Donato JJ. 2021. Novel class 1 integron harboring antibiotic resistance genes in wastewater-derived bacteria as revealed by functional metagenomics. Plasmid 114:102563.

33. Solis MN, Loaiza K, Torres-Elizalde L, Mina I, Šefcová MA, Larrea-Álvarez M. 2024. Detecting Class 1 Integrons and Their Variable Regions in Escherichia coli Whole-Genome Sequences Reported from Andean Community Countries. Antibiotics 13:394.

34. Cantón R, González-Alba JM, Galán JC. 2012. CTX-M Enzymes: Origin and Diffusion. Front Microbiol 3:110.

35. Schwarz S, Kehrenberg C, Doublet B, Cloeckaert A. 2004. Molecular basis of bacterial resistance to chloramphenicol and florfenicol. FEMS Microbiol Rev 28:519–542.

36. Wang Z, Lu Q, Mao X, Li L, Dou J, He Q, Shao H, Luo Q. 2022. Prevalence of Extended-Spectrum β-Lactamase-Resistant Genes in Escherichia coli Isolates from Central China during 2016–2019. Animals 12:3191.

37. Graham DW, Bergeron G, Bourassa MW, Dickson J, Gomes F, Howe A, Kahn LH, Morley PS, Scott HM, Simjee S, Singer RS, Smith TC, Storrs C, Wittum TE. 2019. Complexities in understanding antimicrobial resistance across domesticated animal, human, and environmental systems. Ann N York Acad Sci 1441:17–30.

38. Zheng W, Huyan J, Tian Z, Zhang Y, Wen X. 2020. Clinical class 1 integron-integrase gene – A promising indicator to monitor the abundance and elimination of antibiotic resistance genes in an urban wastewater treatment plant. Environ Int 135:105372.

39. Larsson DGJ, Flach C-F. 2022. Antibiotic resistance in the environment. Nat Rev Microbiol 20:257–269.

40. Cui C-Y, Li X-J, Chen C, Wu X-T, He Q, Jia Q-L, Zhang X-J, Lin Z-Y, Li C, Fang L-X, Liao X-P, Liu Y-H, Hu B, Sun J. 2022. Comprehensive analysis of plasmid-mediated tet(X4)-positive Escherichia coli isolates from clinical settings revealed a high correlation with animals and environments-derived strains. Sci Total Environ 806:150687.

41. Murray M, Salvatierra G, Dávila-Barclay A, Ayzanoa B, Castillo-Vilcahuaman C, Huang M, Pajuelo MJ, Lescano AG, Cabrera L, Calderón M, Berg DE, Gilman RH,

Tsukayama P. 2021. Market Chickens as a Source of Antibiotic-Resistant Escherichia coli in a Peri-Urban Community in Lima, Peru. Front Microbiol 12:635871.

Supplementary Materials

Extended Methods

Biological reagents preparation

Total DNA purification: Total DNA was extracted from an *E. coli* culture grown to OD_{600} = 0.7 using the Quick DNA Miniprep kit (Cat # D4069, Zymo Research) following the manufacturer's protocol. DNA was quantified using a NanoDrop spectrophotometer and stored at -20°C.

Oligo design: To identify resistance genes, all available *E. coli* resistance gene sequences in GenBank as of January 2022 were collected. Individual alignments for *blaCTX-M-15* and *floR* were performed using AliView and MUSCLE, focusing on conserved regions [1,2] (Supplementary Dataset 1 and Dataset 2, respectively). The resulting sequences were 1057 bp for *blaCTX-M-15* and 1415 bp for *floR*. Primer sets were designed for the *blaCTX-M-15* [3] and *floR* [4] genes. For crRNA guide design and evaluation, CRISPRscan, Chop-Chop, and RNAfold bioinformatics tools were used [5 – 7]. Primers and crRNA sequences were sourced from Macrogen Inc. (Seoul, South Korea). crRNA was synthesized by *in vitro* transcription using the TranscriptAid T7 High Yield Transcription Kit (#K0411, ThermoFisher Scientific) and purified with the RNA Clean & Concentrator Kit (Cat #11-353B, Zymo Research).

crRNA production: crRNAs were produced by *in vitro* transcription using T7 RNA polymerase. Double-stranded constructs were designed to include the T7 promoter, an adaptor, and complementary crRNA sequences (Table 1). *In vitro* transcription of the dsDNA templates yielded a range of 3000 to 9000 pmoles of RNA transcript per 50 µL reaction, with concentrations ranging from 61 to 160 µM, sufficient for 4 to 12 thousand assays.

Enzymes production: Taq DNA polymerase and Cas12a proteins were sourced from locally expressed and purified stocks stored at -80°C, as detailed in [8]. Our standardized protocol yields approximately 23 mg of Taq DNA polymerase and 78 mg of Cas12a per 1 L of induced culture. Stock concentrations of 24.5 µM for Taq DNA polymerase and 18.8 µM for Cas12a were used in this study.

Antimicrobial susceptibility test

Disk diffusion: The antibiotic susceptibility profile of 32 *E. coli* isolates was determined by the disk diffusion method, using *E. coli ATCC* 25922 (Cat # 0335, Lab Elite) as the control strain [9]. *E.coli* isolates from glycerol stocks were streaked on LB agar plates and incubated overnight at 37°C. Isolated colonies were resuspended in 0.9% saline solution to a density of 0.5 McFarland and swabbed onto Mueller-Hinton agar plates (Cat # M173-500G, Himedia). Antibiotic disks, including cefotaxime (CTX) 30 µg (Cat # 9017, Liofilchem), and ceftazidime (CAZ) 30 µg (Cat # 9019, Liofilchem) were placed on the surface of the medium. After 18 hours of incubation at 37°, inhibition zones were measured and interpreted following the CLSI guidelines. A confirmatory test for ESBL production was performed using CTX 30 µg and CAZ 30 µg disks combined with clavulanic acid: CTX/AC 40 µg (Cat # 9182, Liofilchem), and CAZ/AC 40 µg (Cat # 9145, Liofilchem). Plates were incubated for 18 hours at 37°C, and ESBL producers were detected by measuring the difference in the inhibition halo of the antibiotic in the presence of clavulanic acid (>5 mm) [9].

Microdilution assay: Florfenicol (Cat #F1427-500MG, Merck) was dissolved in dimethyl sulfoxide (DMSO) to a concentration of 100 mg/ml. Serial dilutions, ranging from 256 µg/ml to 0.125 µg/ml were prepared in a 96-well plate (Cat # 3596, ThermoFisher) using Mueller- Hinton Broth II (Cat # 610218, Liofilchem) [10]. Each

well was inoculated with 1.5 X 10^6 CFU/ml of cells. After 18 h of incubation at 37°C, the MIC was determined. The breakpoint for discriminating susceptible from resistant isolates was 32 µg/mL [11].

Bioinformatic analysis

DNA sequencing data were downloaded from the BioProject web portal of the NCBI (https://www.ncbi.nlm.nih.gov/bioproject/) using accession code PRJNA821865. ARG presence was evaluated using the ResFinder platform (http://genepi.food.dtu.dk/resfinder) v4.6.0 [12] with default parameters. Briefly, a minimum length of 60% and a threshold of 90% were set up for ARG and disinfectant-resistance gene identification. *E.coli* was defined as the species input. For the identification of the integrase-integron class 1, the VRprofile2 platform (https://tool2-mml.sjtu.edu.cn/VRprofile/) [13] and the IntegronFinder tool (v2.0.5) [14] on the Galaxy EU server (https://usegalaxy.eu/) were used simultaneously with default parameters.

Data Analysis and Software

Fluorescence data from the Synergy H1 plate reader were collected using Gen 5 software and exported to Excel. NF_{ntc} values were calculated during data processing and analysis as appropriate. All fluorescence data analysis and chart preparation were performed using GraphPad Prism version 10.0.0 for Windows, www.graphpad.com.

Supplementary figures

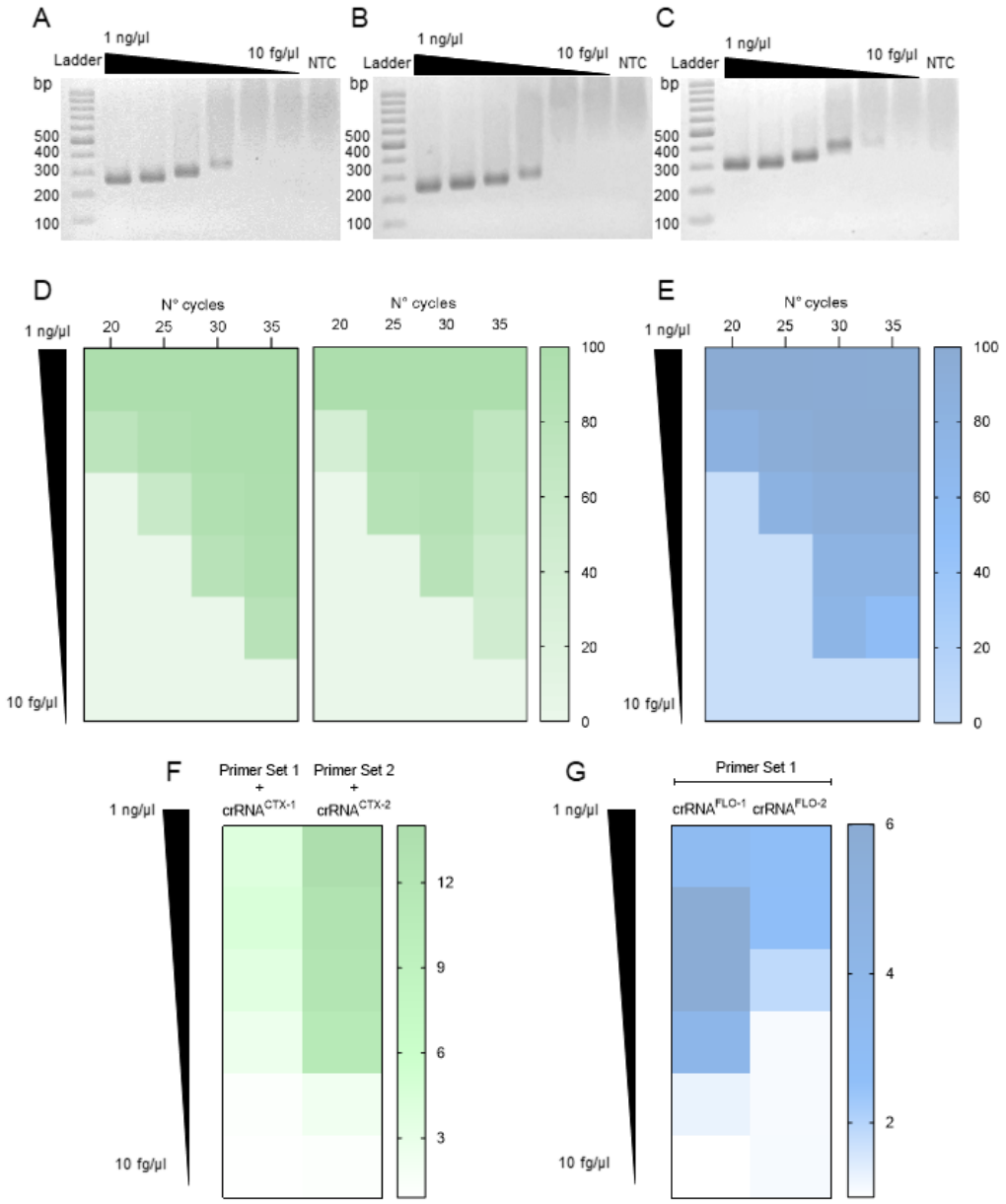

Supplementary Figure 1. Overview of the optimization process for the CRISPR/Cas12a detection systems. (A), (B), and **(C)** show agarose gel images illustrating the results of the 30-cycle PCR for the *blaCTX-M-15* primer set 1, primer set 2, and the *floR* primer set, respectively. The observed decrease in migration with reduced fragment concentration is attributed to an interaction with the SYBR Gold dye, as documented in the literature [15]. **(D)** Heatmap displaying the AUC (Area Under the Curve) values of the amplification bands observed in an agarose gel for the *blaCTX-M-*

15 primer sets. A template titration was conducted in a standard PCR with an increasing number of amplification cycles. **(E)** Similar to (D), but for the *floR* primer set. **(F)** Heatmap displaying fluorescent ratio values for the crRNA candidates designed for the *blaCTX-M-15* gene, obtained from CRISPR-Cas-based detection of 30-cycle PCR amplification products across a template concentration range from 10 fg/µl to 1 ng/µl. **(G)** Similar to (F), but for *floR*.

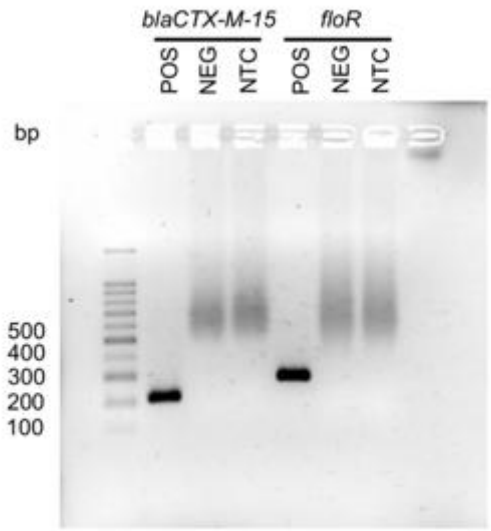

Supplementary Figure 2. Agarose gel displaying PCR amplification products for the ARG evaluated. Amplified products obtained from a standard 30-cycle PCR were analyzed using 1.7% agarose gel electrophoresis, with a 100 bp ladder for size reference. Amplicons were observed exclusively in positive samples. POS indicates a reaction containing the target gene; NEG indicates a reaction with template DNA missing the target gene; NTC indicates a reaction without template DNA. Specifically, the primer set 2 targeting the *blaCTX-M-15* gene produced a 216 bp amplicon, while the gene-specific primer for *floR* produced a 270 bp amplicon.

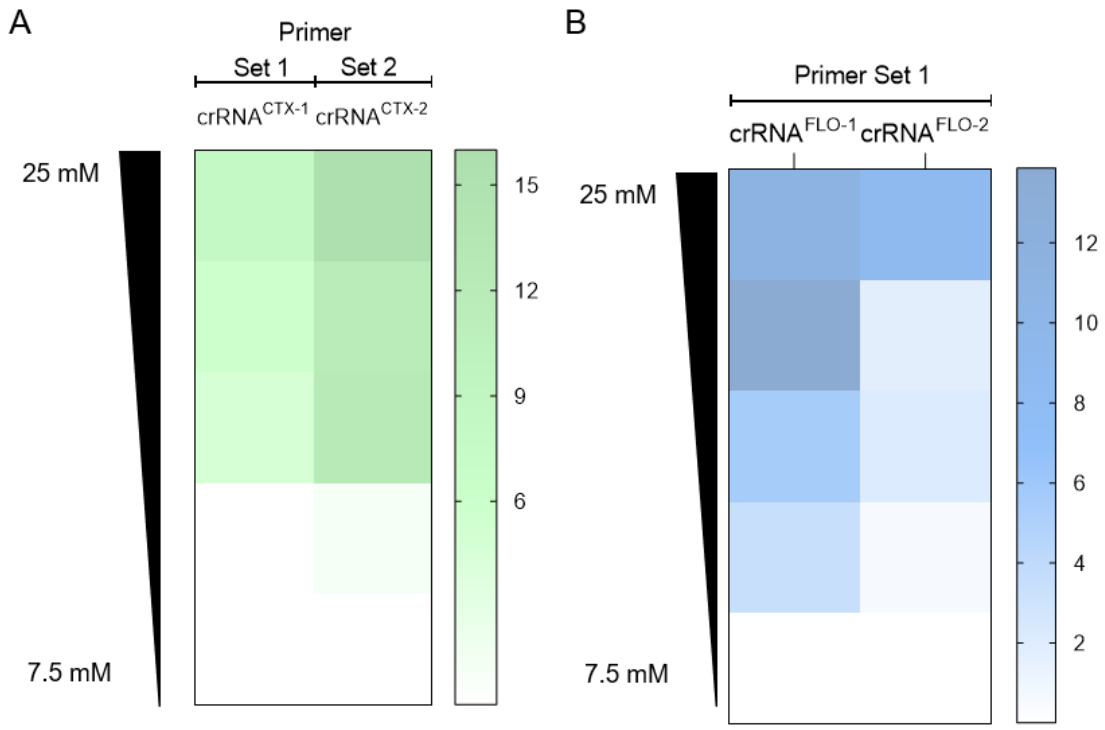

Supplementary Figure 3. Evaluation of Mg2+ concentration on the CRISPR-Cas system performance. Heatmaps displaying the NF_{NTC} values of the $MgCl^{2+}$ titration for the crRNA candidates designed for *blaCTX-M-15* and *floR*. The concentrations ranged from 7.5 to 25 mM. PCR amplicons were obtained using a 30-cycle PCR protocol with primer set 2 for *blaCTX-M-15* and primer set 1 for *floR*. The NF_{NTC} values were measured at 15 min.

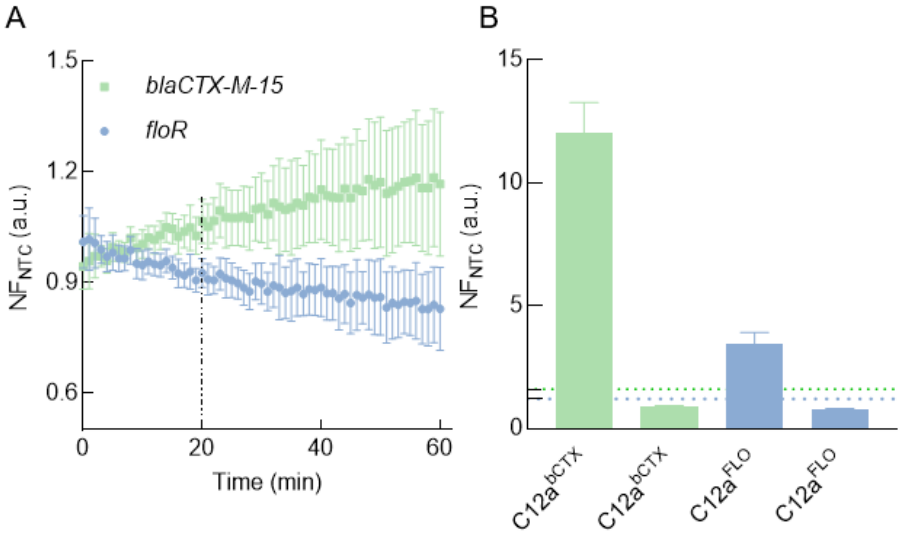

Supplementary Figure 4. Determination of Limit of Blank (LoB) and Day-to-Day Reproducibility of C12a^{bCTX} and C12a^{FLO} (A) Normalized fluorescence ratio (NF_{NTC}) values over time (minutes) for ten negative samples were analyzed to determine the Limit of Blank (LoB). The average NF_{NTC} values for negative samples after 20 minutes (dotted line) were 1.04 ± 0.02 for *blaCTX-M-15* and 0.94 ± 0.02 for *floR*. Error bars represent the standard deviation of at least ten consecutive measurements. **(B)** NF_{NTC} values for positive and negative samples at 20 minutes detection point across 34 experimental days. The bar represents the mean NF_{NTC} values with the error bars representing the standard deviation. The dotted lines correspond to the LoB values calculated for each gene.

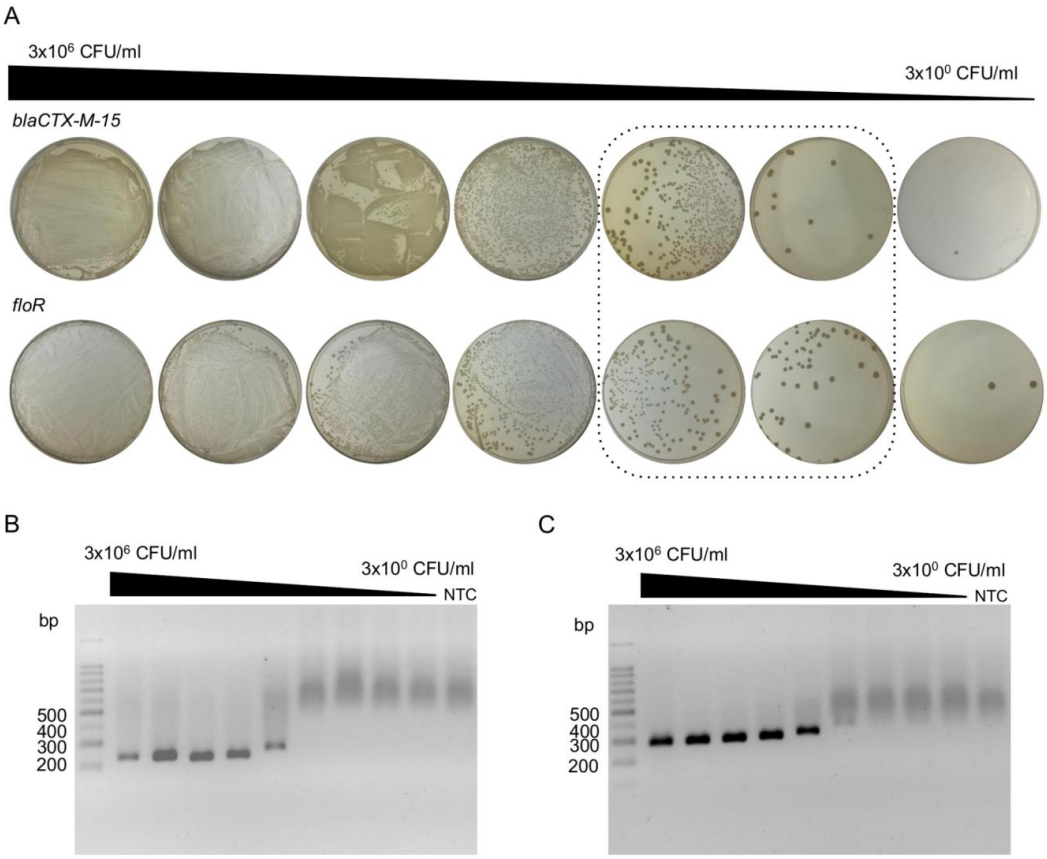

Supplementary Figure 5. Determination of the Limit of detection based on CFU quantification. To determine the LoD in CFU/ml, 7 ten-fold dilutions of a cell culture of *E.coli* ATCC25922 at 0.5 Mc Farland were prepared. **(A)** *E.coli* cells were plated on LB agar after 18 hours of incubation at 37°C. The dilution curve was prepared using 1 mL of LB medium, and 50 µL of each dilution was spread on the LB plates. The CFU/ml titer was determined using the CFU number observed in the dilutions framed in the dotted box. **(B)** Amplified products obtained from each dilution using a standard 30-cycle PCR were analyzed using 1.7% agarose gel electrophoresis, with a 100 bp ladder for size comparison. For *blaCTX-M-15* an amplicon of 216 bp was expected. **(C)** Similar to panel (B), but for *floR,* with an expected amplicon size of 270 bp. The reduced migration at lower fragment concentrations is caused by an interaction with the SYBR Gold dye, as documented in the literature [15].

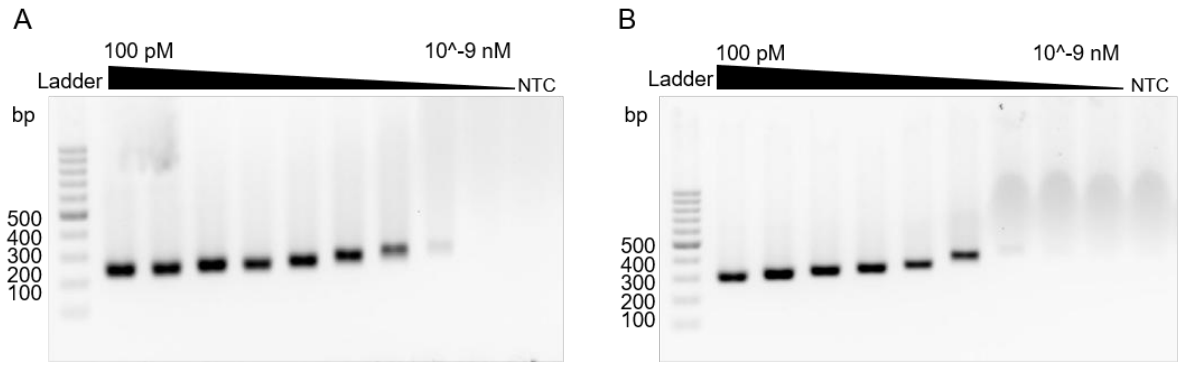

Supplementary Figure 6. Agarose-gel electrophoresis for comparison of analytical sensitivity between CRISPR-Cas-based fluorescent and naked-eye agarose electrophoresis detection. Target amplification across different template concentrations over a 30-cycle PCR. Amplified products were resolved using 1.7% agarose gel electrophoresis, alongside a 100 bp ladder for size comparison. **(A)** An amplicon of 216 bp was expected for *blaCTX-M-15*. **(B)** Same as (A), but for *floR* with an expected amplicon size of 270 bp. The observed decrease in migration with reduced fragment concentration is attributed to an interaction with the SYBR Gold dye, as documented in the literature [15].

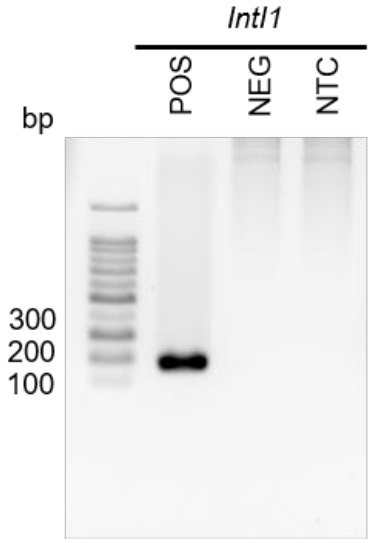

Supplementary Figure 7. Agarose gel displaying PCR amplification products for the *intI1* gene. Amplified products obtained from a standard 30-cycle PCR were analyzed using 1.7% agarose gel electrophoresis, with a 100 bp ladder for size reference. Amplicons were observed exclusively in positive samples. Specifically, the primer set targeting the *intI1* gene produced a 146 bp amplicon.

References

1. Larsson A. AliView: A fast and lightweight alignment viewer and editor for large datasets. Bioinformatics. 2014 Feb 27;30(22):3276–8.
2. Edgar RC. MUSCLE: Multiple sequence alignment with high accuracy and high throughput. Nucleic Acids Res. 2004;32(5):1792–7.
3. Ramadan AA, Abdelaziz NA, Amin MA, Aziz RK. Novel blaCTX-M variants and genotype-phenotype correlations among clinical isolates of extended spectrum beta lactamase-producing Escherichia coli. Sci Rep. 2019 Dec 1;9(1).
4. Qian C, Liu H, Cao J, Ji Y, Lu W, Lu J, et al. Identification of floR Variants Associated With a Novel Tn4371-Like Integrative and Conjugative Element in Clinical Pseudomonas aeruginosa Isolates. Front Cell Infect Microbiol. 2021 Jun 21;11.
5. Moreno-Mateos MA, Vejnar CE, Beaudoin JD, Fernandez JP, Mis EK, Khokha MK, et al. CRISPRscan: Designing highly efficient sgRNAs for CRISPR-Cas9 targeting in vivo. Nat Methods. 2015 Sep 29;12(10):982–8.
6. Labun K, Montague TG, Krause M, Torres Cleuren YN, Tjeldnes H, Valen E. CHOPCHOP v3: Expanding the CRISPR web toolbox beyond genome editing. Nucleic Acids Res. 2019 Jul 1;47(W1):W171–4.
7. Mathews DH. Predicting RNA secondary structure by free energy minimization. Theor Chem Acc. 2006 Aug;116(1–3):160–8.
8. Mendoza-Rojas, G., Sarabia-Vega, V., Sanchez-Castro, A., Tello, L., Cabrera-Sosa, L., Nakamoto, J. A., Peñaranda, K., Adaui, V., Alcántara, R., & Milón, P. (2021). A low-cost and open-source protocol to produce key enzymes for molecular detection assays. *STAR protocols*, 2(4), 100899. https://doi.org/10.1016/j.xpro.2021.100899
9. CLSI. M100 - Performance standards for antimicrobial susceptibility testing. 2020. 282.

10. CLSI. M07 - Methods for Dilution Antimicrobial Susceptibility Tests for Bacteria That Grow Aerobically - Ed12 [Internet]. 12th ed. 2024. Available from: https://clsi.org/terms-of-use/.
11. Singer RS, Patterson SK, Meier AE, Gibson JK, Lee HL, Maddox CW. Relationship between phenotypic and genotypic florfenicol resistance in Escherichia coli. Antimicrob Agents Chemother. 2004;48(10):4047–9.
12. Bortolaia, V., Kaas, R. S., Ruppe, E., Roberts, M. C., Schwarz, S., Cattoir, V., Philippon, A., Allesoe, R. L., Rebelo, A. R., Florensa, A. F., Fagelhauer, L., Chakraborty, T., Neumann, B., Werner, G., Bender, J. K., Stingl, K., Nguyen, M., Coppens, J., Xavier, B. B., Malhotra-Kumar, S., … Aarestrup, F. M. (2020). ResFinder 4.0 for predictions of phenotypes from genotypes. The Journal of antimicrobial chemotherapy, 75(12), 3491–3500. https://doi.org/10.1093/jac/dkaa345
13. Wang, M., Goh, Y. X., Tai, C., Wang, H., Deng, Z., & Ou, H. Y. (2022). VRprofile2: detection of antibiotic resistance-associated mobilome in bacterial pathogens. Nucleic acids research, 50(W1), W768–W773. https://doi.org/10.1093/nar/gkac321
14. Néron, B., Littner, E., Haudiquet, M., Perrin, A., Cury, J., & Rocha, E. P. C. (2022). IntegronFinder 2.0: Identification and Analysis of Integrons across Bacteria, with a Focus on Antibiotic Resistance in Klebsiella. Microorganisms, 10(4), 700. https://doi.org/10.3390/microorganisms10040700
15. Sharp, P. A., Sugden, B., & Sambrook, J. (1973). Detection of two restriction endonuclease activities in Haemophilus parainfluenzae using analytical agarose--ethidium bromide electrophoresis. Biochemistry, 12(16), 3055–3063. https://doi.org/10.1021/bi00740a018

Supplementary files

Supplementary Dataset 1. DNA sequences for *blaCTX-M-15* alignment.

Supplementary Dataset 2. DNA sequences for *floR* alignment.

Supplementary Information:

- Table S1, List of buffers used in this study.
- Table S2, List of oligonucleotides used in this study.
- Table S3, List of DNA sequences for *blaCTX-M-15* and *floR* genes amplified with the selected primer sets. DNA sequences were obtained by SANGER sequencing.
- Table S4, Database with NGS, CRISPR/Cas, and Antimicrobial Susceptibility Testing data for all evaluated samples.
- Table S5, List of ARGs identified in the *blaCTX-M-15* and *floR*-positive *E. coli* isolates, including those found in the genome and in the Class 1 integron.
- Table S6, List of candidate crRNA and primers for additional ARGs detection

Table S1

Buffer	Purpose	Components
RPB 4X	Taq Pol Buffer	200 mM Tris-HCl (pH 8.4 25°C), 300 mM KCl, 12 mM MgCl2, 40% trehalose, 40 mM DTT, 0.4 mM EDTA, 1.6 mM dNTP mix
TBE 5X	Electrophoresis	445 mM Tris Base, 445 mM Boric Acid and 10 mM de EDTA
CRB1	CRISPR Reaction	10 mM TrisHcl – 50 mM NaCl - 100 ug/ul BSA
CRB2		CRB1X – 15 Mm MgCl2
LB	AST test	10 g triptone, 10 g Nacl, 5 g Yeast
LB agar		1 L LB and 15 g agar

Table S2

List of primers						
Gene	**Set**	**Orientation**	**Sequence**	**Amplicon size (bp)**	**ealing temper**	**Source**
blaCTX-M-15	1	Forward	GCAAAAACTTGCCGAATTAGAG	241	56 °C	This study
		Reverse	CTTTTCCGCAATCGGATTATAG			
	2	Forward	GCGCTACAGTACAGCGATAA	216	50 °C	Ramadan et al., 2019
		Reverse	TTTACCCAGCGTCAGATTCC			
floR	1	Forward	GCGCAACGGCTTTCGTCATT	270	58 °C	Qian et al., 2021
		Reverse	GCATCGCCAGTATAGCCAAA			
intI1	1	Forward	GGCTTCGTGATGCCTGCTT	146	59°C	Zhang et al., 2020
		Reverse	CATTCCTGGCCGTGGTTCT			

List of crRNAs					
Gene	**Set**	**PAM**	**Sequence**	**Length**	**Source**
blaCTX-M-15	crRNACTX-1	TTTA	TAATTTCTACTAAGTGTAGATACAGATTCGGTTCGCTTTCACTT	23	This study
	crRNACTX-2	TTTC	TAATTTCTACTAAGTGTAGATGTCTCCCAGCTGTCGGGCGAACG	23	
floR	crRNAFLO-1	TTTA	TAATTTCTACTAAGTGTAGATTGCCAACCGTCCTGAGGGTGTCG	23	
	crRNAFLO-2	TTTG	TAATTTCTACTAAGTGTAGATTCGCTTTCCGTCTACTTCAAGCA	23	
intI1	crRNAINT1	TTTG	TAATTTCTACTAAGTGTAGATAAGGCGCGCTGAAAGGTCTGGTCA	24	
	crRNAINT2	TTTG	TAATTTCTACTAAGTGTAGATCGCAGCACACGCATTCGACCGATC	24	
	crRNAINT3	TTTT	TAATTTCTACTAAGTGTAGATGCGCAGCACACGCATTCGACCGAT	24	

crRNA repeat sequence is highlighted in red.

Table S3

Amplicon sequence obtained by SANGER sequency

Gene	Length	DNA sequence
blaCTX-M-15	184	CAGCGATAACGTGGCGATGAATAAGCTGATTGCTCACGTTGGCGGCCCGGCTAGCGTCAC CGCGTTCGCCCGACAGCTGGGAGACGAAACGTTCCGTCTCGACCGTACCGAGCCGACGTT AAACACCGCCATTCCGGGCGATCCGCGTGATACCACTTCACCTCGGGCAATGGCGCAAAC TCTG
floR	213	GTCATTGCGTCTCTGGGAGCAGCTTGGTCTTCAACTGCACCGGCCTTTGTCGCTTTCCGTCT ACTTCAAGCAGTGGGCGCGTCGGCCATGCTGGTGGCGACGTTCGCGACGGTTCGCGACGTT TATGCCAACCGTCCTGAGGGTGTCGTCATCTACGGCCTTTTCAGTTCGATGCTGGCGTTCGT GCCTGCGCTCGGCCCTATCGCCGGAACA

Database codebook_Table S4

Codebook	Description
1	Positive
0	Negative
CTX	Cefotaxime
CTX/CA	Cefotaxime and clavulanic acid
CAZ	Ceftazidimae
CAZ/CA	Ceftazidime and clavulanic acid
R	Resistant
S	Susceptible

Table S4

Code	Type of sample	NGS	Status	Disk difussion								MIC		CRISPR		LFA	
				CTX (mm)	CTX/CA (mm)	Difference (mm)	Status	CAZ (mm)	CAZ/CA (mm)	Difference (mm)	Status	MIC (µg/ml)	MIC status	Ratio	Status	Bands	Status
bla001	*E.coli* isolate	0	S	30	32	3	S	21	22.0	1	S	na	na	0.8	S	na	na
bla002	*E.coli* isolate	1	R	6	23	17	R	12	21	9	R	na	na	9.1	R	na	na
bla003	*E.coli* isolate	1	R	6	19	13	R	14	18.6	5	R	na	na	13.4	R	na	na
bla004	*E.coli* isolate	0	S	21	24	3	S	24	25.5	1	S	na	na	0.9	S	na	na
bla005	*E.coli* isolate	1	R	9	21	12	R	13	21.2	8	R	na	na	12.8	R	na	na
bla006	*E.coli* isolate	1	R	6	22	15	R	14	21.2	8	R	na	na	12.5	R	na	na
bla007	*E.coli* isolate	0	S	30	31	1	S	31	31.5	1	S	na	na	0.8	S	na	na
bla008	*E.coli* isolate	1	R	7	18	11	R	13	19.3	6	R	na	na	11.7	R	na	na
bla009	*E.coli* isolate	1	R	6	24	18	R	14	22	7	R	na	na	12	R	na	na
bla010	*E.coli* isolate	0	S	19	22	3	S	26	26.2	1	S	na	na	0.8	S	na	na
bla011	*E.coli* isolate	0	S	19	20	1	S	22	23.3	2	S	na	na	1	S	na	na
bla012	*E.coli* isolate	0	S	27	29	2	S	21	23	2	S	na	na	0.9	S	na	na
bla013	*E.coli* isolate	1	R	6	23	17	R	14	21.8	8	R	na	na	12.5	R	na	na
bla014	*E.coli* isolate	0	S	24	26	3	S	21	21.6	1	S	na	na	0.8	S	na	na
bla015	*E.coli* isolate	0	S	26	26	1	S	22	22.8	1	S	na	na	0.9	S	na	na
flo001	*E.coli* isolate	1	R	na	na	na	na	na	na	na	na	>256	R	3.2	R	na	na
flo002	*E.coli* isolate	1	R	na	na	na	na	na	na	na	na	128	R	3.5	R	na	na
flo003	*E.coli* isolate	0	S	na	na	na	na	na	na	na	na	8	S	0.9	S	na	na
flo004	*E.coli* isolate	0	S	na	na	na	na	na	na	na	na	16	S	0.8	S	na	na
flo005	*E.coli* isolate	1	R	na	na	na	na	na	na	na	na	128	R	2.4	R	na	na
flo006	*E.coli* isolate	1	R	na	na	na	na	na	na	na	na	>256	R	3.6	R	na	na
flo007	*E.coli* isolate	1	R	na	na	na	na	na	na	na	na	>256	R	3.7	R	na	na
flo008	*E.coli* isolate	0	S	na	na	na	na	na	na	na	na	128	S	3.3	S	na	na
flo009	*E.coli* isolate	0	S	na	na	na	na	na	na	na	na	>256	S	4	S	na	na
flo010	*E.coli* isolate	0	S	na	na	na	na	na	na	na	na	8	S	0.8	S	na	na
flo011	*E.coli* isolate	1	R	na	na	na	na	na	na	na	na	>256	R	4.2	R	na	na
flo012	*E.coli* isolate	1	R	na	na	na	na	na	na	na	na	>256	R	3.2	R	na	na
flo013	*E.coli* isolate	0	S	na	na	na	na	na	na	na	na	16	S	0.8	S	na	na
flo014	*E.coli* isolate	0	S	na	na	na	na	na	na	na	na	16	S	0.7	S	na	na
flo015	*E.coli* isolate	0	S	na	na	na	na	na	na	na	na	8	S	0.8	S	na	na
flo016	*E.coli* isolate	1	R	na	na	na	na	na	na	na	na	128	R	3.1	R	na	na
flo017	*E.coli* isolate	1	R	na	na	na	na	na	na	na	na	>256	R	3.6	R	na	na
Fbla1	Total DNA	na	na	na	na	na	na	na	na	na	na	na	na	6.2	R	1	R
Fbla2	Total DNA	na	na	na	na	na	na	na	na	na	na	na	na	10.9	R	1	R
Fbla3	Total DNA	na	na	na	na	na	na	na	na	na	na	na	na	1.4	S	0	S
Fbla4	Total DNA	na	na	na	na	na	na	na	na	na	na	na	na	12.4	R	1	R
Fbla5	Total DNA	na	na	na	na	na	na	na	na	na	na	na	na	12.1	R	1	R
Fbla6	Total DNA	na	na	na	na	na	na	na	na	na	na	na	na	7.5	R	1	R
Fbla7	Total DNA	na	na	na	na	na	na	na	na	na	na	na	na	0.9	S	0	S
Fflo1	Total DNA	na	na	na	na	na	na	na	na	na	na	na	na	4.2	R	1	R
Fflo2	Total DNA	na	na	na	na	na	na	na	na	na	na	na	na	5.1	R	1	R
Fflo3	Total DNA	na	na	na	na	na	na	na	na	na	na	na	na	4.8	R	1	R
Fflo4	Total DNA	na	na	na	na	na	na	na	na	na	na	na	na	4.3	R	1	R
Fflo5	Total DNA	na	na	na	na	na	na	na	na	na	na	na	na	3.8	R	1	R
Fflo6	Total DNA	na	na	na	na	na	na	na	na	na	na	na	na	1.3	S	0	S
Fflo7	Total DNA	na	na	na	na	na	na	na	na	na	na	na	na	4.3	R	1	R

Table S5_Summary

Summary ARG found			
aac	aminoglycoside	*antibiotic inactivation*	*3-N-acetyltransferase*
aadA	aminoglycoside	*antibiotic inactivation*	*nucleotidyltransferase*
aph	aminoglycoside	*antibiotic inactivation*	*3'-O-phosphotransferase*
arr	rifamycin/macrolide	*antibiotic inactivation*	*ribosyltransferase*
bla	penam	*antibiotic inactivation*	*beta-lactamase*
cat	phenicols	*antibiotic inactivation*	*acetyltransferase*
cml/mdf	phenicols	*antibiotic efflux*	*efflux pump*
dfrA	trimethoprim	*antibiotic target replacement*	*dihydrofolate reductase*
erm	macrolide	*antibiotic target alteration*	*methyltransferase*
floR	phenicols	*antibiotic efflux*	*efflux pump*
fosA	fosfomycin	*antibiotic inactivation*	*thiol transferase*
lnu	lincosamide	*antibiotic inactivation*	*nucleotidyltransferase*
mcr	polymyxin	*antibiotic target alteration*	*phosphoethanolamine transferase*
mph	macrolide	*antibiotic inactivation*	*phosphotransferase*
qac	disinfectant	*antibiotic efflux*	*efflux pump*
qnr	quinolone	*antibiotic target protection*	*structure mimic*
sul	sulfonamide	*antibiotic target replacement*	*dihydropteroate synthase*
tet	tetracycline	*antibiotic efflux*	*efflux pump*

Table S5

Code	Out of Class 1 integron																			Within Class 1 Integron										MGE near Class 1 Integron	
	aac	*aad*	*aph*	*bla*	*cat*	*cml*	*dfrA*	*erm*	*floR*	*forn*	*fosA*	*lnu*	*mcr*	*mph*	*qac*	*qnr*	*sul*	*tet*	*ABC*	*aac*	*aad*	*ARR*	*bla*	*cat*	*cml*	*dfr*	*lnu*	*qac*	*sul*	Insertion element	Transposons
bla002				*blaCTXM15*		*cmlA*				*formA*						*qnrS1*	*sul2*				*aadA1*					*dfrA1*		*qacE*			
bla003	*aac(3)-IID*			*blaCTXM15*		*cmlA*		*erm(B)*		*formA*				*mph(A)*				*tet(B)*		*aac(6')-Ib-cr*	*aadA5*	*ARR-3*	*blaOXA-1*	*catB3*		*dfrA17*		*qacE*	*sul1*	IS6100	
bla005				*blaCTXM15*		*cmlA*				*formA*						*qnrS1*															
bla006				*blaCTXM15*		*cmlA*				*formA*						*qnrS1*															
bla008				*blaCTXM15*		*cmlA*				*formA*						*qnrS1, qnrB19*	*sul2*				*aadA1*					*dfrA1*		*qacE*			
bla009			*aph(3)-Ia, aph(3)-Ib, aph(6)-Id*	*blaCTXM15, blaTEM176*		*cmlA*				*formA*							*sul2, sul3*	*tet(A)*			*aadA1, aadA2*						*lnu(F)*			*ISEc38*	*TnpR_TnAs1, TnpA_TnAs1*
bla013	*aac(6)-Ib.cr*			*blaCTXM15, blaOXA1*	*catB3*	*cmlA*	*dfrA14*	*erm(B)*		*formA*				*mph(A)*																	
flo001	*aac(3)-Iid*			*blaTEM176, blaCTXM65*		*cmlA*	*dfrA2*		*floR*	*formA*	*fosA*						*sul2, sul3*	*tet(A), tet(M)*			*aadA1, aadA2*				*cmlA1*	*dfrA12*				IS1006, ISVsa3, ISAba33	TnpR_TnShes11, TnpA_TnEcO26
fl002	*aac(3)-Iva*		*aph(4)-Ia*	*blaTEM1B, blaCTXM65*		*cmlA*			*floR*	*formA*						*qnrD1*															
flo005	*aac(3)-Iid*	*aadA2*		*blaTEM176, blaCTXM65*		*cmlA*	*dfrA2*		*floR*	*formA*	*fosA3*	*lnu(F)*					*sul2, sul3*	*tet(A), tet(M)*			*aadA1*				*cmlA1*	*dfrA12*	*lnu(F)*			IS1006, ISVsa3	TnpR_TnShes11, TnpA_TnEcO26
flo006	*aac(3)-Via*		*aph(3)Ib, aph(6)Id, aph(A)IIa*	*blaCMY2, blaCTXM55, blaTEM1B*		*cmlA*			*floR*	*formA*	*fosA3*				*qacE*	qnrB19	*sul1*	*tet(A)*	*sitABC*												
flo007	*aac(3)-IId*		*aph(6)-Id, aph(3)-Ib,*	*blaCTXM65, blaTEM1B*		*cmlA*			*floR*	*formA*	*fosA3*			*mph(A)*				*tet(A)*	*sitABC*		*aadA5*					*dfrA17*		*qacE*	*sul1*	IS6100	TnpR_TnShess11
flo008			*aph(6)-Id, aph(3)-Ib, aph(3)-Iia*	*blaTEM1B, blaCTXM55*		*cmlA*			*floR*	*formA*	*fosA2*	*lnu(G)*					*sul2*	*tet(A), tet(M)*			*aadA2*					*dfrA12*					
flo009	*aac(3)-IIA*			*blaCTXM27*		*cmlA*			*floR*	*formA*	*fosA3*						*sul3*	*tet(A)*	*sitABC*		*aadA1, aadA2*				*cmlA1*						
flo011	*aac(3)-Iva*		*aph(4)-Ia*	*blaTEM1B, blaCTXM65*		*cmlA*			*floR*	*formA*	*fosA3*						*sul2*	*tet(A)*													
flo012	*aac(3)-Iva*		*aph(4)-Ia*	*blaTEM1B, blaCTXM65*		*cmlA*			*floR*	*formA*	*fosA3*						*sul2*	*tet(A)*			*aadA5*					*dfrA17*		*qacE*			
flo016	*aac(3)-Via*		*aph(6)-Id, aph(3)-Ib, aph(3)-Iia*	*blaCMY2, blaCTXM55, blaTEM1B*		*cmlA*			*floR*	*formA*	*fosA3*				*qacE*		*sul1, sul2*	*tet(A)*	*sitABC*												
flo017	*aac(3)-Iid*		*aph(3)-Ia*	*blaCTXM65*		*cmlA*			*floR*	*formA*	*fosA3*		*mcr-1.1*			*qnrS1*	*sul2, sul3*	*tet(A)*			*aadA1*					*dfrA14*	*lnu(F)*				TnpR_TnAs

Table S6

Genes name	crRNA 1	crRNA 2	Primer Forward	Primer Reverse	Reference
aac(6')-Ib-cr	TTTGAGAGGCAAGGTACCGTAACCACC	TTTCTTCTTCCCACCGTCCGTCCCCGCT	TTGCGATGCTCTATGAGTGGCTA	CTCGAATGCCTGGCGTGTTT	A. Robicsek 2006
aadA1	TTTCATCAAGCCTTACGGTCACCGTAA	TTTGTCAGCAAGATAGCCAGATCAATGT	TATCAGAGGTAGTTGGCGTCAT	GTTCCATAGCGTTAAGGTTTCATT	L. P. Randall 2004
aadA2	TTTGTAAGCAGGATAGCTAGATCAATG	TTTCGCTCATCGCCGGCCCAGTCGGGCT	TGTTGGTTACTGTGGCCGTA	GATCTCGCCTTTCACAAAGC	L. P. Randall 2004
aadA5	TTTCCCTGCACAAGTTTTCAAGCAGCTG	TTTGGTACAGCGCTTCAACTGGTCTCAT	AGCTTTTAAGTCGCGTCTTTGT	ACGCAAGATTCTCTCAATCGTT	This study
ARR-3	TTTAAGTCCTCCAACGAATCCAACATTC	TTTCCCGGTAATCCAACACAGTCCTATA	ACATAGTTGAGCCAACAGGACC	GTTTGATGGCTTTGTTATGCAA	This study
blaOXA1	TTTGTGTCCGCACTTACAGGAAACTTG	TTTGATTATGGAAATCAAGACTTCTCTG	TTTTCTGTTGTTTGGGTTTT	TTTCTTGGCTTTTATGCTTG	Sugumar 2014
cmlA1	TTTATTGGCATCACTCGGCATGGACATG	TTTGGCATAAACGGAACTGCTGGCAAGT	TAGTTGGCGGTACTCCCTTG	GAATTGTGCTCGCTGTCGTA	This study
dfrA1	TTTACATCTGACAATGAGAACGTAGTG	TTTGTATATCTCCCCACCACCTGAAACA	TGGTAGCTATATCGAAGAATGGAGT	TATGTTAGAGGCGAAGTCTTGGGTA	M. Grape 2007
dfrA12	TTTCGCAGACTCACTGAGGGAAAAGTC	TTTGATGTACCTCAGATAGAAACATGCC	ACTCGGAATCAGTACGCA	GTGTACGGAATTACAGCT	Guerra 2001
dfrA14	TTTCTTCCCGAGTATTCCAAATACCTT	TTTCTCCGCCACCAGACACTATAACGTG	TTAACCCAGGATGAGAACCT	CGATTGCATAGCTTTGTTAA	Miranda 2016
drfA17	TTTGTCTACTGTTCACGTTGAAGTCGA	TTTGACCCCCGCCAGAGACATATACATG	ACATTTGACTCTATGGGTGTTCTTC	AAAACTGTTCAAAAACCAAATTGAA	M. Grape 2007
sul1	TTTCGCGAGGGTTTCCGAGAAGGTGATT	TTTACAGGAAGGCCAACGGTGGCGCCCA	GCTATTGGTCTCGGTGTCGC	GCATGATCTAACCCTCGGTCT	Zhao 2016
catB3	TTTCCGGACCGTGATGACGTTGATAAGT		AAGGCAAGCTGCTTTCTGAG	GATAAAGGAAGCCCCACTCC	Szczepanowski 2009